



HAL
open science

Exploration of Objects by an Underwater Robot with Electric Sense

Frédéric Boyer, Vincent Lebastard

► **To cite this version:**

Frédéric Boyer, Vincent Lebastard. Exploration of Objects by an Underwater Robot with Electric Sense. Living Machines 2012: Biomimetic and Biohybrid Systems, 2012, barcelone, Spain. pp.50 - 61, 10.1007/978-3-642-31525-1_5 . hal-01503035

HAL Id: hal-01503035

<https://hal.science/hal-01503035v1>

Submitted on 6 Apr 2017

HAL is a multi-disciplinary open access archive for the deposit and dissemination of scientific research documents, whether they are published or not. The documents may come from teaching and research institutions in France or abroad, or from public or private research centers.

L'archive ouverte pluridisciplinaire **HAL**, est destinée au dépôt et à la diffusion de documents scientifiques de niveau recherche, publiés ou non, émanant des établissements d'enseignement et de recherche français ou étrangers, des laboratoires publics ou privés.

Exploration of objects by an underwater robot with electric sense.

Frédéric Boyer and Vincent Lebastard

F. Boyer and V. Lebastard are with IRCCyN-Ecole des Mines de Nantes, 4, rue Alfred Kastler B.P. 20722, 44307, Nantes Cedex 3, France.

Abstract. In this article, we propose a solution to the underwater exploration of objects using a new sensor inspired from the electric fish. The solution is free of any model and is just based on the combination of elementary behaviors, each of these behaviors being achieved through direct feedback of the electric measurements. The solution is robust, cheap and easy to implement. After, stating and interpreting it, the article ends with a few experimental results consisting in exploring small and large unknown objects.

1 Introduction

In spite of its high potential interest for applications as the exploration of deep seas or the rescue missions in catastrophic conditions, underwater navigation in confined unstructured environments wetted by turbid waters is till today a challenge for robotics. Obviously due to the fluid opacity, vision cannot be used while the jamming caused by the multiple interfering reflections as well as the diffraction by small floating particles considerably increase the problems posed to echolocation by sonar. Pursuing a bio-inspired approach in robotics, we can question nature to learn which solutions could be implemented to solve this difficult problem. In fact, evolution has discovered an original sense well adapted to this situation: the electric sense. Developed by several hundreds of fish who have evolved in parallel on both African and South-American continents, electric sense have been discovered by Lissman in 1958 [1]. In the African fish *Gnathonemus Petersii* for instance (pictured in figure 1-(a)), the fish first polarizes its body with respect to an electric organ discharge (EOD) located at the basis of its tail. This polarization which is applied during a short time-pulse, generates around the fish a dipolar shaped electric field which is distorted by the objects present in its surroundings (see figure 1-(b)). Then, thanks to many electro-receptors distributed along its body, the fish "measures" the distortion of the electric fields and infers an image of its surroundings. Thus, electric sense has a quite narrow but relevant niche since none other sense as vision or sonar can work in these conditions. Thus, understanding and implementing this bio-inspired sense on our technologies would offer the opportunity to enhance the navigation abilities of our today under-water robots. Based on these potential interests, Mc. Iver and co authors have recently exploited

a sensor based on the measurement of the electric potential through electrodes in order to address the problem of electrolocation of small objects through off-line particle filtering [2]. In this case, the sensor reduces its body to a so small surface (two points electrodes between which the difference of potentials is measured) that it does not perturb the electric field produced by another pair of punctual (emitting) electrodes between each the voltage is imposed. In Angels¹[3], another technological solution is proposed to the electric sensing. In this case, the sensor is embedded on a realistic 3D body on which each electrode can be polarized with respect to the others through a given vector of voltage \mathbf{U} . The electric field distortions are then measured through the vector \mathbf{I} of the currents flowing across the electrodes and the measurement mode is then qualified of $U - I$. The first letter standing for the emission (here, a vector of voltage \mathbf{U}), the second, for the reception (here a vector of currents \mathbf{I}), and distinguished from the $U - U$ mode of [4]. In the article here presented we address the problem of the underwater exploration of objects electrically un-transparent with respect to the ambient water. Based on the morphology of the sensor (its symmetries in particular), the solution does not require any model of the environment. At the end, it consists of sensor based feedback loops, or in the language of neurobiology of sensory-motor loops. Each of these loops ensure to the sensor a simple behavior whose the combination allows it to find and explore the objects. By exploration, we here means an orbiting motion around the object. Finally, the article is structured as follows. In section 2 we introduce our experimental set up including a family of sensor said slender and the electro-location test-bed on which the algorithms are developed. In section 3, the electric model of the slender sensors is given, while a control strategy suited to object exploration is dealt with in section 4. Finally, experiments based on this control law are detailed in section 5. The article ends with a conclusion in section 6.

2 The electrolocation test-bed

2.1 Sensor

Based on the $U - I$ measurement principle previously explained, we built a first generation of sensors named "slender probes" due to their high aspect ratio (length/thickness) morphology. On these probes, the macro-electrodes \mathcal{E}_α are rings or hemispheres which are azimuthally divided into an even number of identical measurement electrodes. As an illustrative example, Fig. 2 shows one of this probes where each of the macro-electrodes (except \mathcal{E}_0 located in the tail) is divided into a pair of two identical left-right measurement electrodes (it is consequently named the 7-electrode probe and such that $\mathcal{E}_1 = e_1 \cup e_2, \mathcal{E}_2 = e_3 \cup e_4, \mathcal{E}_3 = e_5 \cup e_6$. In all the following, \mathcal{E}_3 will be named the head electrode, \mathcal{E}_2 , the neck electrode while \mathcal{E}_0 is the tail electrode.

¹ The ANGELS project is funded by the European Commission, Information Society and Media, Future and Emerging Technologies (FET) contract number: 231845.

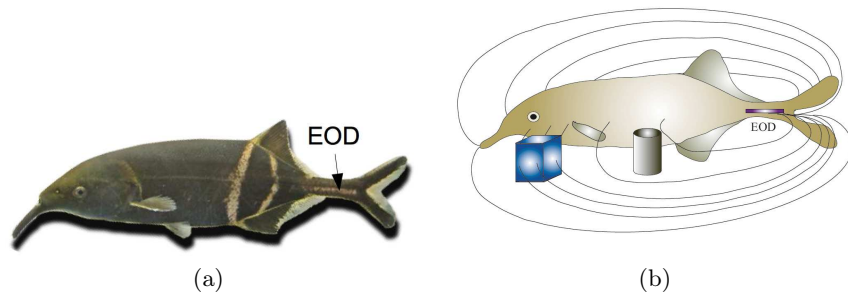


Fig. 1. (Left) The electric fish *Gnathonemus Petersii*. (Right) The electric field is distorted by the presence of an object (for instance, an insulating cylinder pushes the field lines away whereas a conductive cube funnels them).

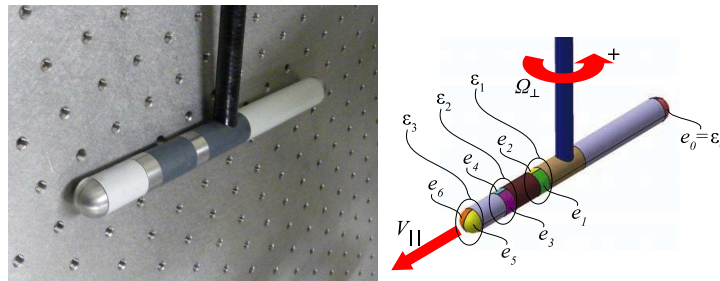


Fig. 2. Picture (left) and schematic view (right) of a 7-electrode sensor organized in 4 polarizable rings, 3 of them being divided in two half rings allowing two lateral (left and right) current measurements.

2.2 Tank and cartesian robot

In order to test our electrolocation sensors and algorithms in controlled and repeatable conditions, an automated test bench consisting in a tank of one cubic meter side with insulating walls and a three-axis cartesian robot has been built (see Fig. 3). The robot fixed on top of the aquarium allows probes positioning in translation along X and Y with a precision of $1/10\text{mm}$ and the orientation in the (X, Y) plane is adjusted in 0.023° abs using an absolute yaw-rotation stage. All probes tested are positioned in the aquarium at adjustable height using a rigid glass epoxy fibre tube ($\varnothing 14\text{mm}$). This vertical insulating tube allows the passage of electrical cables dedicated to the signals coming from the electrodes to readout electronics (analogue chain + ADC board) without compromising the measurements. The maximum speed available is 300mm/s ($\simeq 1\text{km/h}$) for both translations and $80^\circ/\text{s}$ ($13.5\text{tr}/\text{min}$) for rotation.

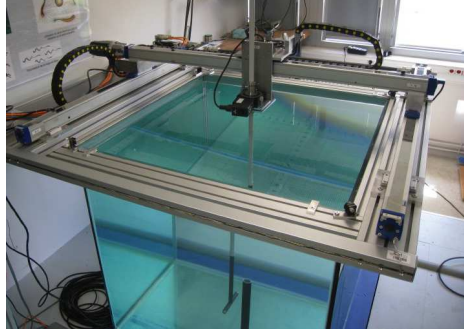


Fig. 3. Electrolocation test bench.

2.3 Objects and scenes

To investigate navigation algorithms in quite complex scenes using electric sense, a set of test objects has been fabricated with conductive and insulating materials. By insulating (or conductive), we mean an ideal material with a conductivity γ such that $\gamma/\gamma_0 = 0$ (or $\gamma/\gamma_0 = \infty$), γ_0 being the conductivity of the ambient fluid (for instance, an ordinary tap water). In practice, plastics (metals) are a good approximation of insulating (conductive) materials. To these simple shaped bodies, we can also add some removable insulating walls. Finally, in the following any scene will be constituted of a combination of these objects and removable walls arbitrarily configured between the four fixed (insulating) walls of the tank.

3 Model

We here restrict our investigations to the case of resistive phenomena. In these conditions, the electric state of a scene can be entirely parameterized by an electric potential ϕ satisfying Laplace equations with boundary conditions imposed on the sensor and wall boundaries as well as crossing boundaries through the objects. In these conditions, reconsidering the principle of the sensor, we first polarize the \mathcal{E}_α ($\alpha \neq 0$) with respect to the ground electrode \mathcal{E}_0 . This is done by imposing the vector of voltages $\mathbf{U} = (U_0, U_1 \dots U_m)^T = (0, U, U \dots U)^T$ with $U_0 = 0$ fixing the ground and U defining the controlled voltage. Then, we measure the vector \mathbf{I} of the currents I_k crossing the e_k for $k = 0, 1, 2 \dots n$. According to the laws of electrostatics [5], they detail as:

$$I_k = \gamma_0 \int_{e_k} \nabla \phi \cdot \mathbf{n} \, ds \quad (1)$$

where we used the Ohm law relating the vector field of currents in the medium \mathbf{j} with the electric field $-\nabla \phi$ and where by convention \mathbf{n} being the inward normal to the sensor, one current is considered positive when

it flows out from the sensor. To this first decomposition of the total currents vector we can add another one which is based on the morphology of the sensor. Indeed, thanks to the symmetries of the sensor, the vector of total currents can be decomposed as a sum of two components named "lateral currents" and "axial currents" as follows:

$$\mathbf{I} = \mathbf{I}_{ax} \oplus \mathbf{I}_{lat}. \quad (2)$$

In (2), \mathbf{I}_{ax} is axi-symmetric whereas the component \mathbf{I}_{lat} is axi-skew-symmetric. In other words, for any of the e_i belonging to a same \mathcal{E}_α , the components $I_{ax,i}$ are identical whereas for a couple of opposed (e_i, e_{i+1}) on a same ring \mathcal{E}_α , we have $I_{lat,i} = -I_{lat,i+1}$. From these considerations of symmetry, it will be easy to extract \mathbf{I}_{lat} and \mathbf{I}_{ax} from \mathbf{I} using the relations:

$$\mathbf{I}_{ax} = \mathbf{D}_+ \mathbf{P}_+ \mathbf{I}, \quad (3)$$

Where \mathbf{P}_+ projects the currents crossing the e_k on those crossing the \mathcal{E}_α , by simply adding all the I_k of a same ring \mathcal{E}_α , that being done ring by ring. Regarding \mathbf{D}_+ , it is the $(n+1) \times (m+1)$ matrix defined by $D_{+(i\alpha)} = A_i/A_\alpha$ if $e_i \subset \mathcal{E}_\alpha$ and $D_{+(i\alpha)} = 0$ otherwise, with A_i and A_α the area of e_i and \mathcal{E}_α respectively. This matrix allows one to equi-distribute the I_α onto the e_k with $e_k \in \mathcal{E}_\alpha$.

In the same manner, we can write:

$$\mathbf{I}_{lat} = \mathbf{D}_- \mathbf{P}_- \mathbf{I}. \quad (4)$$

where, the projection matrix \mathbf{P}_- is such that once applied to $\mathbf{I} = (I_0, I_1, I_2, \dots, I_n)^T$, it gives the reduced vector : $(0, I_2 - I_1, I_4 - I_3, \dots, I_n - I_{n-1})^T$, in the case (always verified) where the numbering of the electrodes e_i ($i > 1$), is such that the (e_i, e_{i+1}) are opposed pairs in the same \mathcal{E}_α . In addition, \mathbf{D}_- allows one to recover the vector of currents \mathbf{I}_{lat} by distributing the $|I_{i+1} - I_i|$ onto the $(n+1)$ e_i slots.

From an expansion in perturbations with respect to the aspect ratio (radius of the sensor over its length) we obtained in [6], the model of the lateral currents as following:

$$\mathbf{I}_{lat} \simeq \mathbf{P}_\perp \nabla_\perp \Phi_1, \quad (5)$$

with:

$$\nabla_\perp \Phi_1 = \left(\int_{e_0} \nabla \phi_1 \cdot \mathbf{n}_\perp ds, \dots, \int_{e_n} \nabla \phi_1 \cdot \mathbf{n}_\perp ds \right)^T \quad (6)$$

the vector of lateral excitation fluxes in which ϕ_1 is the potential reflected by the object once polarized by the sensor, \mathbf{n}_\perp is the lateral component of the normal to the sensor, and \mathbf{P}_\perp is a tensor named tensor of lateral polarizability of the sensor which is diagonal positive at the leading order. As regards the axial currents, we have shown in [6], that we also have at the leading order:

$$\mathbf{I}_{ax} \simeq \mathbf{I}^{(0)} - \mathbf{D}_+ \overline{\mathbf{C}}^{(0)} \Phi_1. \quad (7)$$

with: $\Phi_1 = (\phi_1(\mathbf{x}_{c0}), \dots, \phi_1(\mathbf{x}_{cm}))^T$, the vector of iso-potentials applied by the reflected field by the object on the sensor's electrodes; $\mathbf{I}^{(0)}$ the vector of basal currents, i.e. with no object in the scene; $\overline{\mathbf{C}}^{(0)}$ the conductivity matrix of the sensor with no object in the scene (i.e. such that $\mathbf{I}^{(0)} = \mathbf{D}_+ \overline{\mathbf{C}}^{(0)} \mathbf{U}$). Finally, $\mathbf{I}^{(0)}$, \mathbf{P}_\perp , and $\overline{\mathbf{C}}^{(0)}$ are data intrinsically related to the sensor and the ambient medium with no object. As such, they can be computed once before all through a numerical code as the Boundary-Elements-Method or directly through a preliminary off-line calibration of the sensor. On the other hand, $\nabla_\perp \Phi_1$ and Φ_1 are vectors depending on the geometry of the object and its situation (position-orientation) with respect to the sensor frame.

4 Control law

In this section, we present a control strategy allowing the sensor to explore the objects in its surroundings. This strategy is stated in this section, while we postpone to the next section its physical interpretation.

4.1 General architecture

The general architecture of the underwater robot is decomposed into three elementary blocks as depicted on figure 4. The first block is directly related to the electric measurements of the electric sensor. The second is related to the navigation, and is consequently named "navigator". The last one controls the locomotion of the underwater vehicle on which the sensor is embarked. As a result, it is named "the locomotor". In the following we will concentrate our attention onto the second block which allows the robot to compute the desired (axial) linear and angular (lateral) velocities V_\parallel and Ω_\perp as a function of the electric measurements \mathbf{I} . The navigator, can be decomposed into the following three sub-blocks:

- 1°) A sub-block "axialisation" which extracts the axial component of the currents \mathbf{I}_{ax} from the vector of total currents \mathbf{I} .
- 2°) A sub-block "lateralisation" which extracts the lateral component of currents \mathbf{I}_{lat} from the vector of total currents \mathbf{I} .
- 3°) A sub-block "memorization" which memorizes certain values taken by the measurements along the motion of the sensor.

4.2 Case of the 7-electrode sensor

Before going on with the implementation of this general structure, let us illustrate these three operations with the 7-electrode sensor of figure 2. In this case, the axialisation operator consists of:

$$\mathbf{I}_{ax} = \mathbf{D}_+ \mathbf{P}_+ \mathbf{I} = (I_5 + I_6, I_5 + I_6, I_4 + I_3, I_4 + I_3, I_2 + I_1, I_2 + I_1, I_0)^T \quad (8)$$

Alternatively, we also introduce the vector of reduced axial currents:

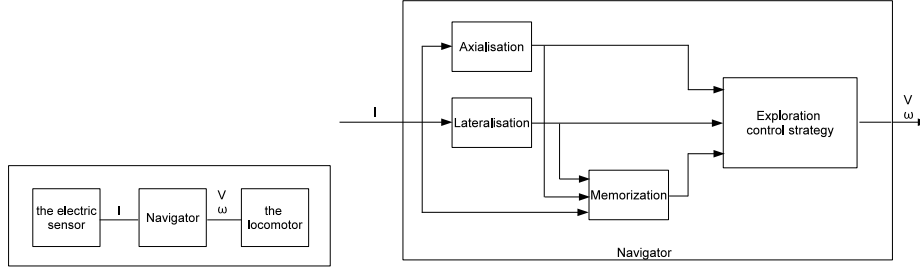


Fig. 4. (Left) The general architecture of the underwater robot. (Right) The navigator.

$$\bar{\mathbf{I}}_{ax} = (I_5 + I_6, I_4 + I_3, I_2 + I_1, I_0)^T \quad (9)$$

where the over-barre indicates that the concerned currents are those flowing across the m rings \mathcal{E}_α . The lateralisation operator allows to obtain the vector of lateral currents :

$$\mathbf{I}_{lat} = \mathbf{D}_P \mathbf{I} = (I_6 - I_5, I_5 - I_6, I_4 - I_3, I_3 - I_4, I_2 - I_1, I_1 - I_2, 0)^T \quad (10)$$

As a first application of the "memorization block" the basal component of the currents $\mathbf{I}^{(0)}$ is memorized in a preliminary calibration phase. By virtue of the symmetry properties of the sensor, this component is purely axial. Thanks to this preliminary calibration, we can compute at any time of the experiment the perturbative axial currents $\delta \mathbf{I}_{ax}$:

$$\delta \mathbf{I}_{ax} = \mathbf{I}_{ax} - \mathbf{I}^{(0)}, \quad (11)$$

which only result from the presence of an object in the scene. We introduce $\delta \bar{\mathbf{I}}_{ax}$ the reduced vector of perturbative currents flowing across the rings. In the same way, the vector of lateral perturbative currents is directly given by $\delta \mathbf{I}_{lat} = \mathbf{I}_{lat}$ since, due to the lateral symmetry of the sensor, the vector of basal currents has no lateral component, i.e.: $\mathbf{D}_P \mathbf{I}^{(0)} = \mathbf{0}$. With these definitions in hand, we are now going to introduce a simple control law ensuring the exploration as previously defined.

4.3 Exploration control strategy

Using the three elementary operations previously introduced, one can derive a control strategy consisting in exploring the objects present in the scene. By "exploring" we here mean "to seek the objects" and "to follow their boundaries without touching them". Such a law is the natural resultant of the combination of three basic behaviors:

- 1°) Seek any object electrically contrasted with respect to the ambient medium.

- 2°) Flee from the electric influence of the object.
- 3°) Follow the boundaries of the object.

Now, let us reveal how these three behaviors can be easily obtained through simple sensory-motor loops. The two first ones are in fact produced by applying a feedback control law of the head lateral currents of the general form:

$$V_{\parallel} = cte > 0, \quad \Omega_{\perp} = K \delta I_{lat,1}, \quad (12)$$

with K a gain ensuring the sensor to be attracted by any un-transparent object when $K = k/\delta\bar{I}_{ax,1}$ and to be repulsed by any object when $K = k/|\delta\bar{I}_{ax,1}|$ with $k > 0$ in both cases. As regards the third behavior, it is simply obtained by applying the control law:

$$V_{\parallel} = cte > 0, \quad \Omega_{\perp} = k' (\delta\bar{I}_{ax,1} - \delta\bar{I}_{ax,1}^{(mem)}), \quad (13)$$

where the axial velocity V_{\parallel} is ruled by the same constant value as in (12), while $k' > 0$ is a constant gain. In (13), $\delta\bar{I}_{ax,1}^{(mem)}$ represents a value of the axial head current stored by the memorizing block of figure 4 at a time of the motion where it has a remarkable evolution (typically when it attains an extremum). Thus, beyond this time, $\delta\bar{I}_{ax,1}^{(mem)}$ represents a desired value that the sensor will track along its motion.

4.4 Application to the 7-electrode sensor

We are now going to see how we can combine the three behaviors of section 4.3 in order to achieve the exploration task. Indeed, it suffices to sequentially order the three behaviors along with the three following phases symbolized through the graph of transitions of figure 5-(a) whose the application is schematized on figure 5-(b):

- First phase (from A to B in figure 5): It consists in seeking an electrically non-transparent object by applying the attractive behavior (12) with $K = k/\delta\bar{I}_{ax,1}$ and $k > 0$.
- Second phase (from B to B' in figure 5): This second phase corresponds to the initialization of the orbiting motion of the sensor around the object. It is obtained by applying the repulsive behavior, i.e. (12) with $K = k/|\delta\bar{I}_{ax,1}|$ and $k > 0$.
- Third phase (from B' to C in figure 5): This is the orbiting phase obtained by applying the law (13), in which $\delta\bar{I}_{ax,1}^{(mem)}$ is the value of $\delta\bar{I}_{ax,1}$ measured at the last time of the previous phase.

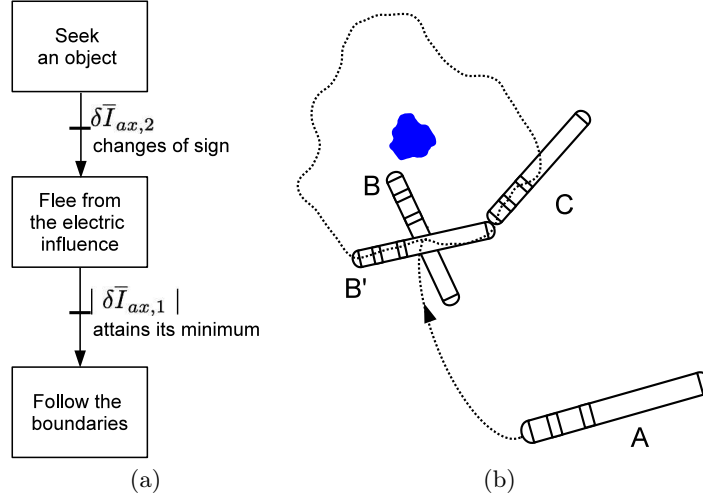


Fig. 5. (a) Sequential graph of exploration task. (b) typical scenario of the object exploration.

As indicated on the sequential graph of figure 5-(a), the commutation between these phases is ruled by the following events which only depend time variation of the measurements (and not of their magnitude). Indeed, the commutation from phase 1 to phase 2 is activated by the change of sign of $\delta \bar{I}_{ax,2}$, i.e. when the current flowing across the second ring (neck ring) change of sign. The second transition (from phase 2 to phase 3) is activated when $|\delta \bar{I}_{ax,1}|$ attains its minimum value.

5 Interpretation

Let us now interpret the previous law. First, since due to equations 5 and 6, the lateral current $\delta I_{lat,1} = I_{lat,1}$ is proportional to the lateral flux of the electric field reflected by the object, any law of the general form (12) ensures the sensor to align its head on the electric field lines. This first condition is ensured while the sensor moves with the constant axial velocity. As a result, since all the electric lines (integral of the reflected electric field) emanate from the objects close to the sensor, the sensor is attracted or repulsed by them depending of the sign of the gain K in (12). Finally, the presence of $|\delta \bar{I}_{ax,1}|$ in (12) allows to normalize the control as the sensor approaches a targeted object. When it is applied in the first phase, the sensor is attracted by the objects. When getting closer and closer to an object, the sensor faces it and more and more electric field lines are captured by the object if it is conductive. Thus, the electric field lines are funneled on the front (head) electrode. On the contrary, if the object is insulating the electric field lines are pushed backward along the sensor axis. As a result, when the sensor approaches an object, the current lines go from the head to the neck electrode if the

object is and insulator and from the neck to the head if it is a conductor (see figure 6). Thus, in both cases it happens a time when $\delta\bar{I}_{ax,2}$ changes of sign. This is at this time that the control law commutes from the attractive to the repulsive behavior. When this occurs, the sign of K in (12) is changed and the sensor starts to avoid the object, this is done till the $|\delta\bar{I}_{ax,1}|$ attains its minimum which means that the tail (\mathcal{E}_0) and the head electrodes are equidistant from the object. Indeed, when one of these two electrodes is closer to the object than the other, the electric lines emitted by the tail or the lines received by the head are more perturbed (than in the equidistant case) and the corresponding measurement $|\delta\bar{I}_{ax,1}|$ is larger (see figure 6). Finally, as this condition is satisfied, $\delta\bar{I}_{ax,1}$ is memorized as a reference that the sensor try to maintain. That corresponds to follow an iso current around the sensor, this last condition ensuring the following of the object boundaries.

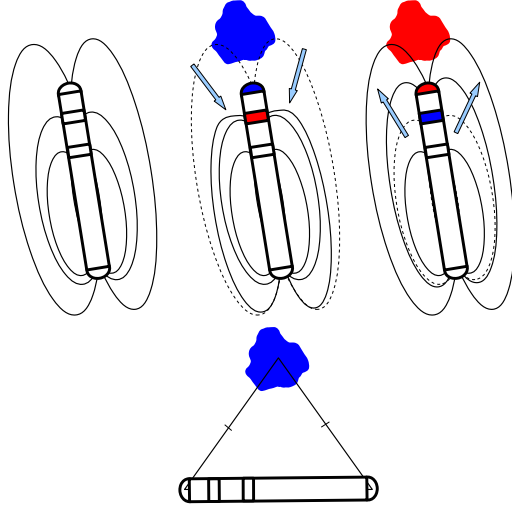


Fig. 6. (Top) The electric lines are pushed forward and backward depending if the object facing the sensor is conducting or insulating. (Bottom) When the head and tail electrodes are equidistant of the object, the head currents attain a minimum.

6 Experimental results

In this section, we report some of the experimental results illustrating the previous exploration control strategy. The electric feedback loops (12) and (13) are tuned once for all with $k = 50V_{\parallel}$ and $k' = 2,5V_{\parallel}$, and then applied to all the tests. The experimental conditions are those described in section 2. For each experiment the sensor first starts and seek the object, second, it flees from the electric influence of the object and third, follows the boundaries of the object. Many trials have been

successfully achieved with this single simple law. We here report three of them, the first one illustrating the exploration of a small object while the second and the third are applied to the exploration of large objects. In the first case, the explored object is a conducting ellipsoid. Figure 7 (Top) displays the trajectory of the sensor when the sensor orbits around the ellipsoid. Note that while the sensor trajectory is near to be elliptic, this elliptic orbit displays an angular shift with respect to the elliptic boundary of the object. This shift is probably due to the initial conditions of the orbit while the aspect ratio of the elliptic trajectory (great over small axis) should be an image of that of the object. Finally, the case of the exploration of large objects is illustrated on the two last examples figure 8, the first object is an insulating wall placed in the middle of the tank and the second is simply the bound walls of the tank. In the last case, while the sensor is orbiting around the tank, a piece of insulating wall is placed on one of the tank corners (bottom-left). When moving past this corner, the sensor does follow the new piece of wall. Figure 8 (Bottom) shows the time evolution of the measured currents along the sensor trajectory in the case where it follows the tank walls. The two time transitions of the sequential graph (5-a) are pointed by B and B' as in figure (5-b).

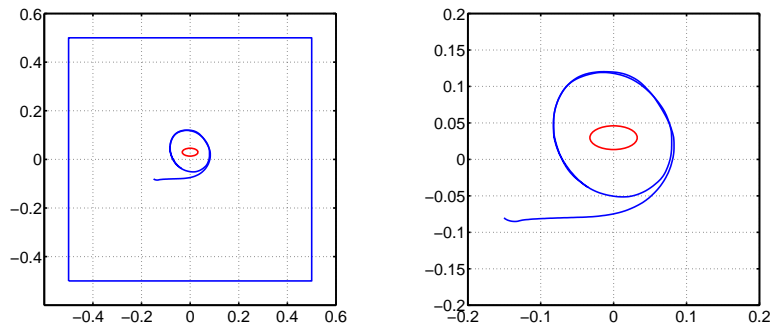


Fig. 7. Exploration of a conducting ellipsoid.

7 Conclusion

In this article we have addressed the problem of object exploration using a sensor bio-inspired of electric fish. The solution is free from any model of the sensor electric interactions with the surrounding. It allows seeking any object electrically contrasted with respect to the ambient water and then to turn around. This behavior will be exploited in future to infer a geometric model of the object. Today, it has shown its robustness in many situations with many different objects. In spite of these first success, many other questions today remain. In particular, since the use

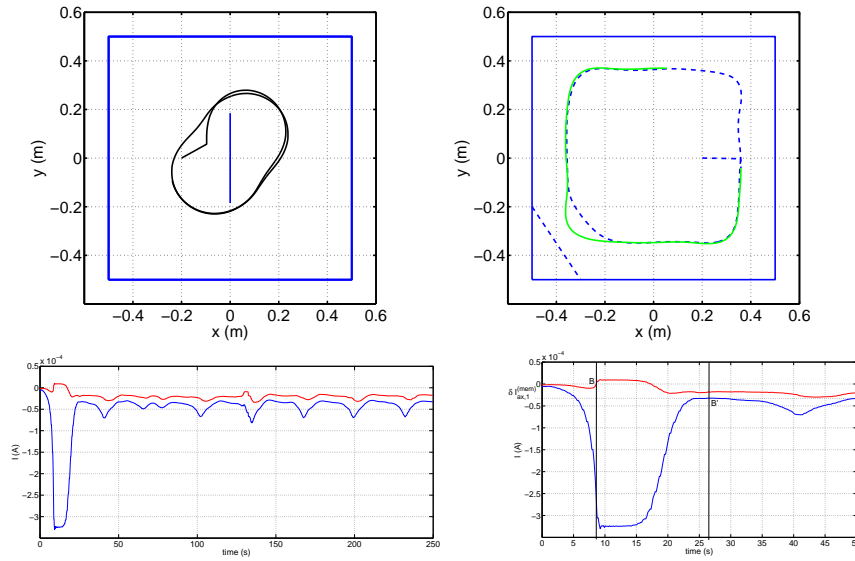


Fig. 8. (Top) Exploration of large objects. (Bottom) Time evolution of the currents $\delta \bar{I}_{ax,1}$ (blue) and $\delta \bar{I}_{ax,2}$ (red) along the sensor path when the sensor follows the tank walls.

of the model is replaced by the morphology of the sensor, the following question arises. In which proportion the sensor morphology determines its behavior with respect to the explored objects. For instance, the distance between the head and neck rings determines the distance at which the sensor detects the presence of an object.

References

1. Lissmann, H., Machin, K.: The mechanism of object location in *Gymnarchus niloticus* and similar fish. *The Journal of Experimental Biology* **35** (1958) 451–486
2. Solberg, J., Lynch, K., MacIver, M.: Active electrolocation for underwater target localization. *The International Journal of Robotics Research* **27** (2008) 529–548
3. the angels project: <http://www.theangelsproject.eu> (2009)
4. Solberg, J., Lynch, K., MacIver, M.: Robotic electrolocation: Active underwater target localization. In: *International Conference on Robotics and Automation*. (2007) 4879–4886
5. Jackson, J.D.: *Classical Electrodynamics* 3rd edition. John Wiley and Sons (1999)
6. Boyer, F., Gossiaux, P., Jawad, B., Lebastard, V., M.Porez.: Model for a sensor bio-inspired by electric fish. *IEEE transactions on robotics* **28**(2) (2012) 492–505